

Estimation of Fiber Orientations Using Neighborhood Information

Chuyang Ye, Jiachen Zhuo, Rao P. Gullapalli, and Jerry L. Prince

Abstract Diffusion magnetic resonance imaging (dMRI) has been used to noninvasively reconstruct fiber tracts. Fiber orientation (FO) estimation is a crucial step in the reconstruction, especially in the case of crossing fibers. In FO estimation, it is important to incorporate spatial coherence of FOs to reduce the effect of noise. In this work, we propose a method of FO estimation using neighborhood information. The diffusion signal is modeled by a fixed tensor basis. The spatial coherence is enforced in weighted ℓ_1 -norm regularization terms, which contain the interaction of directional information between neighbor voxels. Data fidelity is ensured by the agreement between raw and reconstructed diffusion signals. The resulting objective function is solved using a block coordinate descent algorithm. Experiments were performed on a digital crossing phantom, ex vivo tongue dMRI data, and in vivo brain dMRI data for qualitative and quantitative evaluation. The results demonstrate that the proposed method improves the quality of FO estimation.

1 Introduction

Diffusion magnetic resonance imaging (dMRI) has been used to noninvasively reconstruct fiber tracts by imaging the anisotropy of water diffusion in tissue [11]. A major topic in dMRI is the estimation of fiber orientations (FOs), especially

C. Ye (✉)

Brainnetome Center, Institute of Automation, Chinese Academy of Sciences, Beijing, China

Department of Electrical and Computer Engineering, Johns Hopkins University, Baltimore, MD, USA

e-mail: chuyang.ye@nlpr.ia.ac.cn

J. Zhuo • R.P. Gullapalli

Department of Radiology, University of Maryland School of Medicine, Baltimore, MD, USA

J.L. Prince

Department of Electrical and Computer Engineering, Johns Hopkins University, Baltimore, MD, USA

in situations where fibers cross. For example, constrained spherical deconvolution [17], q -ball reconstruction [6], multi-tensor models [3, 10, 20], and spherical ridgelet models [13] have been proposed to estimate crossing FOs.

Successful resolution of crossing FOs may require a large number of diffusion gradient directions, which takes a long acquisition time and limits the use in clinical practice [4]. To reduce the required number of gradient directions, with the assumption that the number of FOs in a voxel is small, methods have been proposed to model the diffusion signals using a basis and solve the FO estimation with sparsity regularization [5, 10, 12, 13, 15, 20]. For example, the basis can be diffusion tensors [5, 10, 15, 20], spherical ridgelets [13], or spherical polar Fourier basis [12].

Besides sparsity assumption, it is also important to consider spatial coherence of FOs to reduce the effect of noise and improve FO estimation. For example, in [2] the diffusion weighted images (DWIs) are smoothed before FO estimation whereas in [16] smoothing of FOs is performed after FO estimation. Several works have placed spatial regularization of tensors on the multi-tensor model to estimate FOs, but the sparsity assumption was not used [7, 14]. There are also methods that have combined spatial continuity with sparsity and seek to simultaneously estimate and smooth FOs. In [13], the TV-norm of DWIs is incorporated in the objective function for FO estimation. In [15] and [20], spatial consistency of FOs is enforced by adding the smoothness of the mixture fraction of each basis tensor as regularization terms in the FO estimation. However, in [15] and [20], the FO coherence is ensured in a relatively indirect way in the sense that directional information in FOs is not explicitly modeled in the objective functions. FO estimation incorporating both sparsity and spatial coherence is still an open problem.

In this work, we propose a method of FO estimation using both sparsity assumption and neighborhood information. The diffusion signal is modeled by a fixed tensor basis. In contrast to previous works, we directly incorporate the directional information in the neighborhood into the objective function to encode spatial coherence. Spatial coherence and sparsity are enforced in weighted ℓ_1 -norm regularization terms, which contain the interaction of directional information between neighbor voxels. Data fidelity is ensured by the agreement between raw and reconstructed diffusion weighted signals. The resulting objective function is solved using a block coordinate descent algorithm. Experiments were performed on a digital crossing phantom, ex vivo tongue dMRI data, and in vivo brain dMRI data for evaluation.

2 Methods

2.1 Background: Multi-Tensor Model with a Fixed Tensor Basis

As discussed in [8], the diffusion weighted signal at each voxel can be modeled using a unified framework,

$$S(\mathbf{q}) = S_0 \int_{\mathcal{M}} f(x)R(\mathbf{q}, x)dx, \quad (1)$$

where \mathcal{M} is a smooth manifold, x is a point on \mathcal{M} , $S(\mathbf{q})$ is the diffusion weighted signal with the diffusion gradient \mathbf{q} , S_0 is the signal without diffusion weighting, $R(\mathbf{q}, x)$ is a kernel function, and $f(x)$ is a probability density function. As in [10] and [20], we use a fixed tensor basis to represent diffusion signals, which has the advantage of explicit relationship between the basis and FOs. In this work, the basis comprises $N = 289$ prolate tensors \mathbf{D}_i whose primary eigenvectors (PEVs) \mathbf{v}_i are approximately evenly oriented over the sphere. Each \mathbf{D}_i represents an FO given by its PEV \mathbf{v}_i . The eigenvalues ($\lambda_1 \geq \lambda_2 \geq \lambda_3 > 0$) determine the shape of the basis tensor, and they are determined by examining the diffusion tensors of a noncrossing fiber tract [10].

With this tensor basis, we have $\mathcal{M} = \mathcal{S}^2$ (a unit sphere), $x = \mathbf{v}$ (a unit vector), $f(\mathbf{v}) = f_i \delta(\mathbf{v}; \mathbf{v}_i)$, and $R(\mathbf{q}, \mathbf{v}_i) = e^{-\mathbf{q}^T \mathbf{D}_i \mathbf{q}}$ [8]. If we normalize the diffusion gradient as $\tilde{\mathbf{q}} = \mathbf{q}/|\mathbf{q}|$, then $\tilde{\mathbf{q}}$ is associated with a constant b determined by the imaging sequence. Then, taking noise $n(\mathbf{q})$ into account, (1) becomes [10]

$$S(\mathbf{q}) = S_0 \sum_{i=1}^N f_i e^{-b\tilde{\mathbf{q}}^T \mathbf{D}_i \tilde{\mathbf{q}}} + n(\mathbf{q}), \quad (2)$$

where f_i ($\sum_i f_i = 1$) is the unknown nonnegative mixture fraction (MF) for \mathbf{D}_i .

By defining $y(\mathbf{q}) = S(\mathbf{q})/S_0$ and $\eta(\mathbf{q}) = n(\mathbf{q})/S_0$, (2) can be written as

$$\mathbf{y} = \mathbf{G}\mathbf{f} + \boldsymbol{\eta}, \quad (3)$$

where $\mathbf{y} = (y(\mathbf{q}_1), y(\mathbf{q}_2), \dots, y(\mathbf{q}_K))^T$ (K is the number of DWIs), \mathbf{G} is a $K \times N$ matrix comprising the attenuation terms $G_{ki} = e^{-b\tilde{\mathbf{q}}_k^T \mathbf{D}_i \tilde{\mathbf{q}}_k}$, $\mathbf{f} = (f_1, f_2, \dots, f_N)^T$, and $\boldsymbol{\eta} = (\eta(\mathbf{q}_1), \eta(\mathbf{q}_2), \dots, \eta(\mathbf{q}_K))^T$. Because the number of FOs in each voxel is small, it makes sense to estimate the MFs using sparse reconstruction:

$$\hat{\mathbf{f}} = \arg \min_{\mathbf{f} \geq \mathbf{0}, \|\mathbf{f}\|_1=1} \|\mathbf{G}\mathbf{f} - \mathbf{y}\|_2^2 + \beta \|\mathbf{f}\|_0. \quad (4)$$

By relaxing the constraint of $\sum_{i=1}^N f_i = 1$ and replacing the ℓ_0 -norm with the ℓ_1 -norm [10, 20], we have

$$\hat{\mathbf{f}} = \arg \min_{\mathbf{f} \geq \mathbf{0}} \|\mathbf{G}\mathbf{f} - \mathbf{y}\|_2^2 + \beta \|\mathbf{f}\|_1, \quad (5)$$

Then, the estimated \mathbf{f} is projected onto the unit sphere $\|\mathbf{f}\|_1 = 1$ by normalization [10]. Basis directions with nonzero MFs are interpreted as estimated FOs. Thus, we will use FO estimation and MF estimation interchangeably.

2.2 FO Estimation Using Neighborhood Information

Because of image noise, it is important to incorporate spatial coherence of FOs to improve FO estimation [13]. An intuitive way of incorporating neighborhood information can be based on the smoothness of MFs [15, 20]. But establishing smooth MFs does not mean that the FO angles are smooth. For example, let $\mathbf{f}_a = (1, 0, \dots, 0)^T$, $\mathbf{f}_b = (0, 1, 0, \dots, 0)^T$, and $\mathbf{f}_c = (0, 0, 1, 0, \dots, 0)^T$. The difference between \mathbf{f}_a and \mathbf{f}_b ($\|\mathbf{f}_a - \mathbf{f}_b\|$) is the same as that between \mathbf{f}_a and \mathbf{f}_c ($\|\mathbf{f}_a - \mathbf{f}_c\|$), while the desired difference is clearly related to the basis directions represented by the nonzero entries in the MFs. In this work, we seek to explicitly incorporate the directional information from neighbor voxels into FO estimation.

FO Estimation with Known Neighborhood Information First we consider a simplified case of estimating FOs in a single voxel with known neighbor information. Let the MFs at voxel m be \mathbf{f}_m . A voxel n is in the neighborhood N_m of m and has FOs $\{\mathbf{v}_{n,j}\}_{j=1}^{V_n}$, where V_n is the number of FOs at n . Suppose $\{\mathbf{v}_{n,j}\}_{j=1}^{V_n}$ were known, and we want to estimate \mathbf{f}_m given the neighbor FOs.

We assume that a majority of neighbor voxels $n \in N_m$ have similar FO patterns as the desired one at m . Then, a set of *likely FO* $\{\mathbf{u}_{m,p}\}_{p=1}^{U_m}$ for m can be obtained from the neighbor voxels (details will be introduced later), where U_m is the number of likely FOs at m . Motivated by Ye et al. [18], where fixed pre-determined prior directions at each voxel are encoded in the sparse reconstruction of FOs from dMRI, a weighted ℓ_1 -norm regularized least squares problem derived from a Bayesian perspective can be solved to encode the information of likely FOs:

$$\hat{\mathbf{f}}_m = \arg \min_{\mathbf{f}_m \geq \mathbf{0}} \|\mathbf{G}\mathbf{f}_m - \mathbf{y}_m\|_2^2 + \beta \|\mathbf{C}_m \mathbf{f}_m\|_1. \quad (6)$$

Here, \mathbf{C}_m is a diagonal weighting matrix encoding likely FOs. The basis directions closer to likely FOs are weighted less in the weighted ℓ_1 -norm, and thus they are less penalized in the objective function. We set the diagonal entries as

$$C_{m;ii} = \left(1 - \alpha \max_p |\mathbf{v}_i \cdot \mathbf{u}_{m,p}|\right) / \min_q \left(1 - \alpha \max_p |\mathbf{v}_q \cdot \mathbf{u}_{m,p}|\right), \quad (7)$$

where $\alpha \in [0, 1)$ is a constant. Since \mathbf{v}_i and $\mathbf{u}_{m,p}$ are unit vectors, $0 \leq |\mathbf{v}_i \cdot \mathbf{u}_{m,p}| \leq 1$ and $C_{m:ii}$ is positive. In this way, the penalty for basis directions that are closest to likely FOs is the same as that when no information on likely FOs is used.

Note that our application of FO estimation with spatial coherence is fundamentally different than [18] in two aspects: (1) likely FOs are computed based on neighbor FOs while in [18] an anatomical atlas is needed to provide prior directions specified at each voxel; (2) since the FOs in the neighbors are also to be estimated, voxelwise FO estimation in (6) is inappropriate. The proposed approach to likely FO computation and FO estimation is introduced below.

Likely FO Computation At voxel m we first consider one neighbor voxel n . Between each basis direction \mathbf{v}_i and the neighbor n , we define a *basis-neighbor similarity* $r_m(i, n) = w_{m,n} \max_j |\mathbf{v}_i \cdot \mathbf{v}_{n,j}|$. Here, $w_{m,n}$ is a weighting coefficient, which represents the similarity between m and n . It is defined as $w_{m,n} = e^{-\mu d^2(\mathbf{D}_m, \mathbf{D}_n)}$ (μ is a constant). \mathbf{D}_m and \mathbf{D}_n are the diffusion tensors fitted from DWIs at m and n , respectively, and $d(\mathbf{D}_m, \mathbf{D}_n)$ is a distance metric for tensors \mathbf{D}_m and \mathbf{D}_n : $d(\mathbf{D}_m, \mathbf{D}_n) = \sqrt{\text{Trace}\{\log(\mathbf{D}_m) - \log(\mathbf{D}_n)\}^2}$ [1]. For each \mathbf{v}_i , the max function in $r_m(i, n)$ measures the similarity between \mathbf{v}_i and its closest FO in n , and this similarity is further weighted by the voxel similarity $w_{m,n}$. In this way, given one neighbor n , we can measure how similar \mathbf{v}_i is to the FOs at n .

To consider all neighbor voxels, an *aggregate basis-neighbor similarity* for \mathbf{v}_i at voxel m is defined as $R_m(i) = \sum_{n \in N_m} r_m(i, n)$. We can extract likely FOs for m by finding the basis directions with local maximal R_m values:

$$\{\mathbf{u}_{m,p}\}_{p=1}^{U_m} = \{\mathbf{v}_i | R_m(i) \geq R_m(j), \forall j \neq i : \arccos(|\mathbf{v}_i \cdot \mathbf{v}_j|) \leq \frac{\theta\pi}{180^\circ}\}. \quad (8)$$

Here, θ is a threshold and we empirically choose $\theta = 20^\circ$.

FO Estimation for All Voxels With the likely FOs, the weighting matrix can then be obtained. Note that we have assumed known neighbor information to obtain (6). However, the FOs in the neighbors are also to be estimated. Thus the FOs in all the voxels should be estimated simultaneously. For a total number of M voxels of interest, where the MFs $\mathbf{f} = (\mathbf{f}_1^T, \mathbf{f}_2^T, \dots, \mathbf{f}_M^T)^T$ (and thus the FOs) are unknown, the FO estimation can be achieved as

$$\hat{\mathbf{f}} = \arg \min_{\mathbf{f} \geq \mathbf{0}} E(\mathbf{f}) = \arg \min_{\mathbf{f}_1, \mathbf{f}_2, \dots, \mathbf{f}_M \geq \mathbf{0}} \sum_{m=1}^M \|\mathbf{G}\mathbf{f}_m - \mathbf{y}_m\|_2^2 + \beta \|\mathbf{C}_m \mathbf{f}_m\|_1. \quad (9)$$

Note that \mathbf{C}_m contains the interaction between neighbors and it is also dependent on α . Greater α leads to more influence from neighbors. β controls the sparsity. In this work, α and β were chosen empirically.

2.3 Minimization of the Objective Function

Because each voxel m is coupled with its neighbors in \mathbf{C}_m in (9), we use a block coordinate descent (BCD) optimization strategy. At iteration $k + 1$,

$$\begin{aligned}\hat{\mathbf{f}}_m^{k+1} &= \arg \min_{\mathbf{f}_m \geq \mathbf{0}} E(\hat{\mathbf{f}}_1^{k+1}, \dots, \hat{\mathbf{f}}_{m-1}^{k+1}, \mathbf{f}_m, \hat{\mathbf{f}}_{m+1}^k, \dots, \hat{\mathbf{f}}_M^k) \\ &= \arg \min_{\mathbf{f}_m \geq \mathbf{0}} \|\mathbf{G}\mathbf{f}_m - \mathbf{y}_m\|_2^2 + \beta \|\mathbf{C}_m^{k+1} \mathbf{f}_m\|_1.\end{aligned}\quad (10)$$

Using (8), the likely FOs $\mathbf{u}_{m,p}^{k+1}$ are obtained by finding the local maxima from $R_m^{k+1}(i) = \sum_{n \in N_m} w_{m,n} \max_j |\mathbf{v}_i \cdot \mathbf{v}_{n,j}^{k+1} \mathbb{1}_{n < m}|$, where $\mathbb{1}$ is an indicator function. Then, \mathbf{C}_m^{k+1} can be determined with $\mathbf{u}_{m,p}^{k+1}$ using (7).

To solve (10), we define $\mathbf{g}_m^{k+1} = \mathbf{C}_m^{k+1} \mathbf{f}_m$. Since \mathbf{C}_m^{k+1} is diagonal and $C_m^{k+1:ii} > 0$, \mathbf{C}_m^{k+1} is invertible and $\mathbf{f}_m = (\mathbf{C}_m^{k+1})^{-1} \mathbf{g}_m^{k+1}$. By defining $\tilde{\mathbf{G}}_m^{k+1} = \mathbf{G}(\mathbf{C}_m^{k+1})^{-1}$,

$$\hat{\mathbf{g}}_m^{k+1} = \arg \min_{\mathbf{g}_m^{k+1} \geq \mathbf{0}} \|\tilde{\mathbf{G}}_m^{k+1} \mathbf{g}_m^{k+1} - \mathbf{y}_m\|_2^2 + \beta \|\mathbf{g}_m^{k+1}\|_1.\quad (11)$$

We find $\hat{\mathbf{g}}_m^{k+1}$ using the method in [9] and the MFs are estimated as

$$\hat{\mathbf{f}}_m^{k+1} = (\mathbf{C}_m^{k+1})^{-1} \hat{\mathbf{g}}_m^{k+1}.\quad (12)$$

Then, we project $\hat{\mathbf{f}}_m^{k+1}$ back onto the unit sphere by normalization: $\tilde{\mathbf{f}}_{m,i}^{k+1} = \hat{\mathbf{f}}_{m,i}^{k+1} / \sum_j \hat{\mathbf{f}}_{m,j}^{k+1}$, and the FOs at m at iteration $k + 1$ are the basis directions with $\tilde{\mathbf{f}}_{m,i}^{k+1} > t$ ($t = 0.1$ in this work), because FOs with small MFs are interpreted as components of isotropic diffusion [10, 18].

The FOs are initialized by Landman et al. [10]. Iterative update is terminated if the FO difference between successive iterations is small or the maximum iteration is reached.

3 Experiments

3.1 3D Digital Crossing Phantom

A 3D digital crossing phantom was generated to simulate two tracts crossing at 90° , where one b_0 image and 30 gradient directions ($b = 700 \text{ s/mm}^2$) were used. Rician noise ($\sigma/S_0=0.05$) was added to the DWIs.

The proposed method with $(\alpha, \beta, \mu) = (0.4, 0.5, 1.0)$ was compared with BEDPOSTX [3] and CFARI [10], which are commonly used with around 30

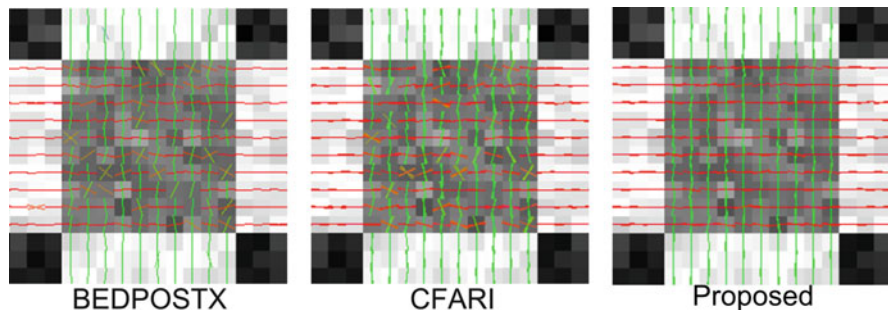


Fig. 1 FO estimation overlaid on the FA map of the 3D crossing phantom

Table 1 The mean errors of FO estimation (with standard deviations in parentheses)

	Noncrossing region		Crossing region	
	e_1	e_2	e_1	e_2
BEDPOSTX	3.26° (3.58°)	2.80° (1.89°)	12.12° (8.92°)	13.72° (11.66°)
CFARI	3.41° (1.73°)	0.79° (1.88°)	12.23° (7.79°)	12.21° (11.52°)
Proposed	3.08° (1.63°)	0.58° (1.64°)	5.57° (2.24°)	3.89° (2.65°)

gradient directions. The results are overlaid on the fractional anisotropy (FA) map in Fig. 1. Compared with BEDPOSTX and CFARI, the proposed method produces smoother FOs and better identifies crossing FOs. We then compared the results quantitatively by using the two error measures proposed in [18], where the first measure (e_1) represents how close each estimated FO is to its ground truth FO, and the second one (e_2) measures how accurately each ground truth FO is represented. The results are listed in Table 1. The proposed method estimates FOs more accurately in both noncrossing and crossing regions.

3.2 Real Data

Ex Vivo Tongue dMRI Nine b_0 images and 64 gradient directions ($b = 2000 \text{ s/mm}^2$) were acquired on a 3T MRI scanner (Magnetom Trio, Siemens, Erlangen, Germany). The resolution is 2 mm isotropic.

The proposed method with $(\alpha, \beta, \mu) = (0.4, 0.5, 3.0)$ was compared with q -ball imaging (QBI) using spherical harmonics based transformation [6] and CFARI [10]. The eigenvalues of the basis tensors are $\lambda_1 = 7.0 \times 10^{-4} \text{ mm}^2/\text{s}$ and $\lambda_2 = \lambda_3 = 3.0 \times 10^{-4} \text{ mm}^2/\text{s}$. We focus on the crossing region of the genioglossus (GG) and transverse (T) muscle in Fig. 2, where the proposed method better estimates the crossing FOs and produces smoother FOs than QBI and CFARI.

In Vivo Brain dMRI Two b -values ($b = 1000 \text{ s/mm}^2$ and 2000 s/mm^2) were used in the acquisition. Each b -value is associated with 30 gradient directions and

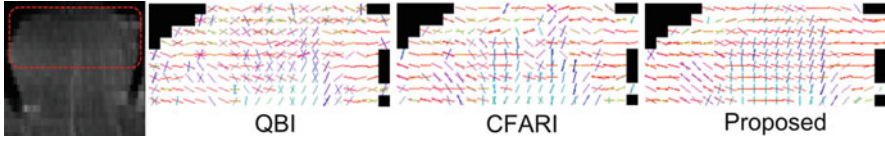


Fig. 2 FO estimation on the ex vivo tongue in the coronal view, which is focused on the crossing of the GG and T muscle (the tongue area is indicated by the white mask). A high resolution structural image (*left*) is shown for location reference

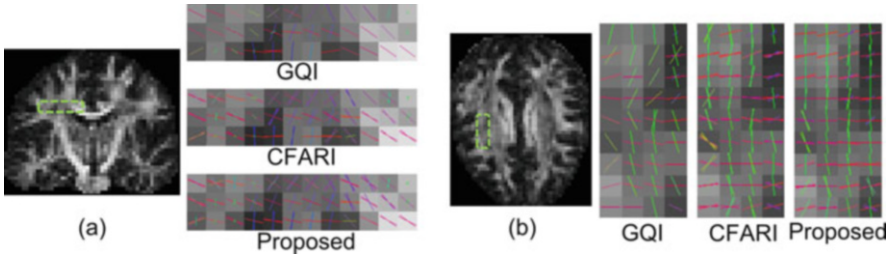


Fig. 3 FO estimation on brain dMRI (overlaid on the FA map), which is focused on the crossing of (a) CC and CST (coronal view) and (b) CC and SLF (axial view)

each DWI has two repeated scans. Twelve b_0 images were also acquired. The images were acquired on a 3T MRI scanner (Magnetom Trio, Siemens, Erlangen, Germany). The resolution is 2.7 mm isotropic.

The proposed method with $(\alpha, \beta, \mu) = (0.4, 0.5, 1.0)$ was compared with CFARI [10] and generalized q -sampling imaging (GQI) [19]. GQI is a generalization of QBI [6] and can reconstruct FOs from multi-shell (multiple b -values) dMRI. The eigenvalues of the basis tensors are $\lambda_1 = 2.0 \times 10^{-3} \text{ mm}^2/\text{s}$ and $\lambda_2 = \lambda_3 = 5.0 \times 10^{-4} \text{ mm}^2/\text{s}$. We highlight two regions for evaluation: the crossing region of the corpus callosum (CC) and the corticospinal tract (CST) and the crossing region of CC and the superior longitudinal fasciculus (SLF), which are shown in Fig. 3. It can be seen that the proposed method is able to better reconstruct the crossing FOs and has smoother results than CFARI and GQI.

4 Conclusion

We have proposed an FO estimation algorithm using neighborhood information. The diffusion signal is modeled by a tensor basis. Directional information in neighbors is modeled in weighted ℓ_1 -norm regularization terms to ensure spatial coherence. FO estimation is achieved using a BCD strategy. The proposed method was applied to simulated and real dMRI data. The results indicate that the proposed method improves FO estimation by using neighborhood information.

Acknowledgements This work is supported by NIH/NINDS 5R01NS056307, and NIH/NINDS IR21NS082891.

References

1. Arsigny, V., Fillard, P., Pennec, X., Ayache, N.: Log-Euclidean metrics for fast and simple calculus on diffusion tensors. *Magn. Reson. Med.* **56**(2), 411–421 (2006)
2. Becker, S., Tabelow, K., Mohammadi, S., Weiskopf, N., Polzehl, J.: Adaptive smoothing of multi-shell diffusion weighted magnetic resonance data by msPOAS. *NeuroImage* **95**, 90–105 (2014)
3. Behrens, T.E.J., Berg, H.J., Jbabdi, S., Rushworth, M.F.S., Woolrich, M.W.: Probabilistic diffusion tractography with multiple fibre orientations: what can we gain? *NeuroImage* **34**(1), 144–155 (2007)
4. Bilgic, B., Setsompop, K., Cohen-Adad, J., Yendiki, A., Wald, L.L., Adalsteinsson, E.: Accelerated diffusion spectrum imaging with compressed sensing using adaptive dictionaries. *Magn. Reson. Med.* **68**(6), 1747–1754 (2012)
5. Daducci, A., Van De Ville, D., Thiran, J.P., Wiaux, Y.: Sparse regularization for fiber ODF reconstruction: from the suboptimality of ℓ_2 and ℓ_1 priors to ℓ_0 . *Med. Image Anal.* **18**(6), 820–833 (2014)
6. Descoteaux, M., Angelino, E., Fitzgibbons, S., Deriche, R.: Regularized, fast, and robust analytical q-ball imaging. *Magn. Reson. Med.* **58**(3), 497–510 (2007)
7. Hao, X., Fletcher, P.: Joint fractional segmentation and multi-tensor estimation in diffusion MRI. In: Gee, J., Joshi, S., Pohl, K., Wells, W., Zillei, L. (eds.) *Information Processing in Medical Imaging. Lecture Notes in Computer Science*, vol. 7917, pp. 340–351. Springer, Berlin (2013). http://dx.doi.org/10.1007/978-3-642-38868-2_29
8. Jian, B., Vemuri, B.C.: A unified computational framework for deconvolution to reconstruct multiple fibers from diffusion weighted MRI. *IEEE Trans. Med. Imaging* **26**(11), 1464–1471 (2007)
9. Kim, S.J., Koh, K., Lustig, M., Boyd, S.: An efficient method for compressed sensing. In: *IEEE International Conference on Image Processing*, vol. 3, pp. 117–120 (2007)
10. Landman, B.A., Bogovic, J.A., Wan, H., ElShahaby, F.E.Z., Bazin, P.L., Prince, J.L.: Resolution of crossing fibers with constrained compressed sensing using diffusion tensor MRI. *NeuroImage* **59**(3), 2175–2186 (2012)
11. Le Bihan, D.: Looking into the functional architecture of the brain with diffusion MRI. *Nat. Rev. Neurosci.* **4**(6), 469–480 (2003)
12. Merlet, S.L., Deriche, R.: Continuous diffusion signal, EAP and ODF estimation via compressive sensing in diffusion MRI. *Med. Image Anal.* **17**(5), 556–572 (2013)
13. Michailovich, O., Rathi, Y., Dolui, S.: Spatially regularized compressed sensing for high angular resolution diffusion imaging. *IEEE Trans. Med. Imaging* **30**(5), 1100–1115 (2011)
14. Pasternak, O., Assaf, Y., Intrator, N., Sochen, N.: Variational multiple-tensor fitting of fiber-ambiguous diffusion-weighted magnetic resonance imaging voxels. *Magn. Reson. Imaging* **26**(8), 1133–1144 (2008). <http://www.sciencedirect.com/science/article/pii/S0730725X08000490>
15. Ramirez-Manzanares, A., Rivera, M., Vemuri, B.C., Carney, P., Mareci, T.: Diffusion basis functions decomposition for estimating white matter intravoxel fiber geometry. *IEEE Trans. Med. Imaging* **26**(8), 1091–1102 (2007)
16. Sigurdsson, G.A., Prince, J.L.: Smoothing fields of weighted collections with applications to diffusion MRI processing. In: *SPIE Medical Imaging*, pp. 90342D–90342D (2014)
17. Tournier, J., Calamante, F., Connelly, A.: Robust determination of the fibre orientation distribution in diffusion MRI: non-negativity constrained super-resolved spherical deconvolution. *NeuroImage* **35**(4), 1459–1472 (2007)

18. Ye, C., Carass, A., Murano, E., Stone, M., Prince, J.L.: A Bayesian approach to distinguishing interdigitated muscles in the tongue from limited diffusion weighted imaging. In: *Bayesian and Graphical Models for Biomedical Imaging. Lecture Notes in Computer Science*, vol. 8677, pp. 13–24. Springer, Berlin (2014)
19. Yeh, F.C., Wedeen, V., Tseng, W.Y.: Generalized q -sampling imaging. *IEEE Trans. Med. Imaging* **29**(9), 1626–1635 (2010)
20. Zhou, Q., Michailovich, O., Rathi, Y.: Resolving complex fibre architecture by means of sparse spherical deconvolution in the presence of isotropic diffusion. In: *SPIE Medical Imaging*, pp. 903425–903425 (2014)